Electronic Supplementary Material (ESI) for Journal of Materials Chemistry C.

Morphology evolution of Eu^{3+}-activated $NaTbF_4$ nanorods: A highly-efficient near-ultraviolet light-triggered red-emitting platform towards application in white light-emitting diode

Peng Du[a,b*†], Weiguan Ran[c†], Weiping Li[ab], Laihui Luo[a,b*] and Xiaoyong Huang[d,e*]

[a]*Department of Microelectronic Science and Engineering, Ningbo University, 315211 Ningbo, China*

[b]*School of Physical Science and Technology, Ningbo University, 315211 Ningbo, China*

[c]*Department of Physics, Pukyong National University, Busan 608-737, South Korea*

[d]*Institute for Advanced Study, Shenzhen University, Shenzhen 518060, China*

[e]*College of Physics and Optoelectronics, Taiyuan University of Technology, Taiyuan 030024, China*

Corresponding authors:

E-mail: dp2007good@sina.com or dupeng@nbu.edu.cn (P. Du); luolaihui@nbu.edu.cn (L. Luo); huangxy04@126.com (X. Huang)

†P. Du and W. Ran contributed equally to this work.

Table S1. Wavenumbers and transition rates for the $^5D_0 \rightarrow {}^7F_J$ (J = 1, 2, 3, 4) of Eu^{3+} ions in $NaTbF_4$:0.3Eu^{3+} nanorods.

Transition	Type	Wavenumber (cm^{-1})	Transition rate (s^{-1})
$^5D_0 \rightarrow {}^7F_1$	Magnetic dipole	16891.89	39.24
$^5D_0 \rightarrow {}^7F_2$	Electric dipole	16233.77	116.96
$^5D_0 \rightarrow {}^7F_3$	Forbidden	15408.32	1.47
$^5D_0 \rightarrow {}^7F_4$	Electric dipole	14347.20	29.94

Table S2. Chromaticity parameters of the fabricated WLEDs device as a function of forward bias current.

Current	*x*	*y*	CCT	CRI
50 mA	0.311	0.354	6430 K	92.1
100 mA	0.307	0.350	6617 K	91.9
150 mA	0.306	0.350	6645 K	91.8
200 mA	0.305	0.348	6746 K	91.7
250 mA	0.302	0.347	6882 K	91.6

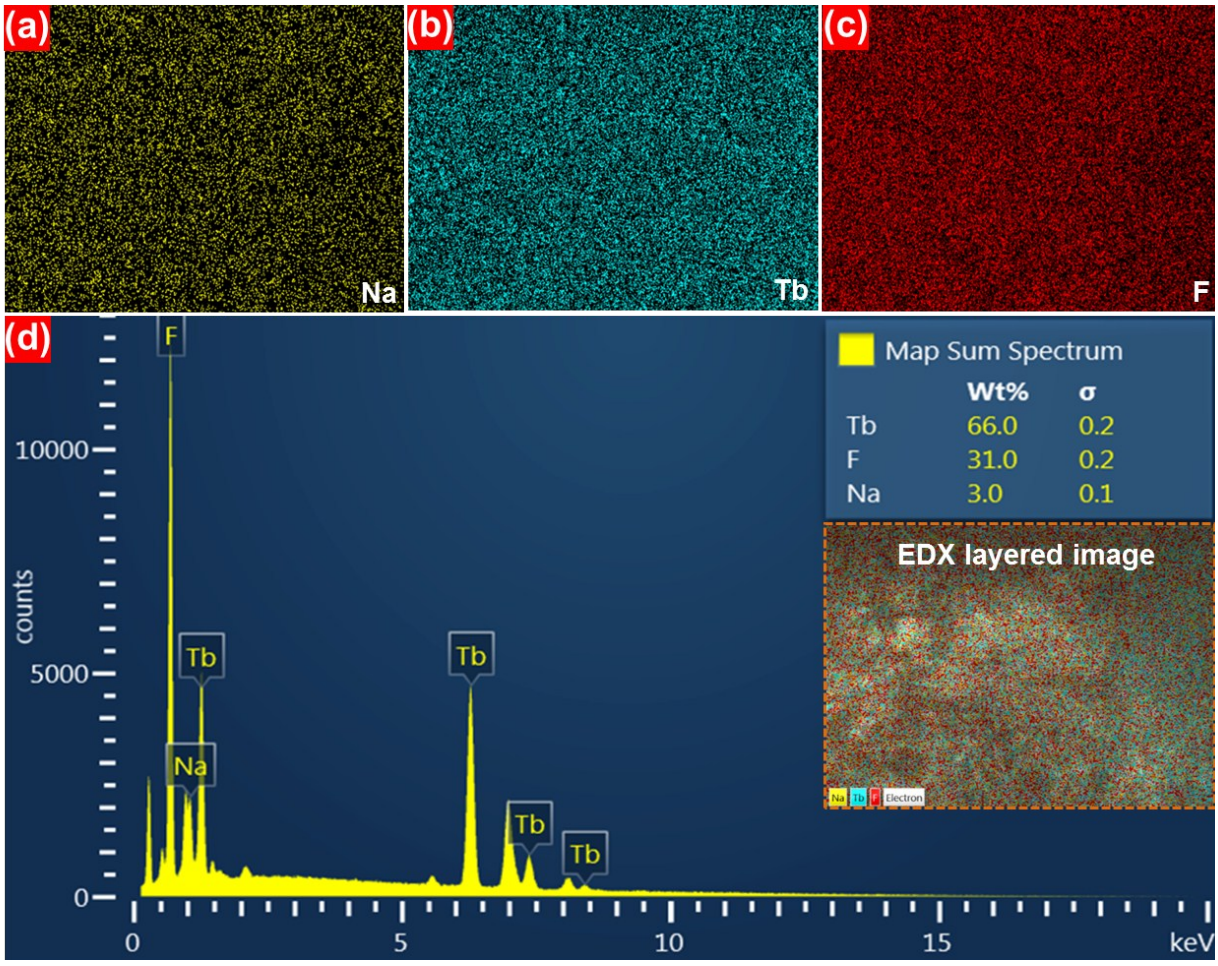

Figure S1. (a)-(c) Elemental mapping and (d) EDX spectrum of the $NaTbF_4$ nanorods.

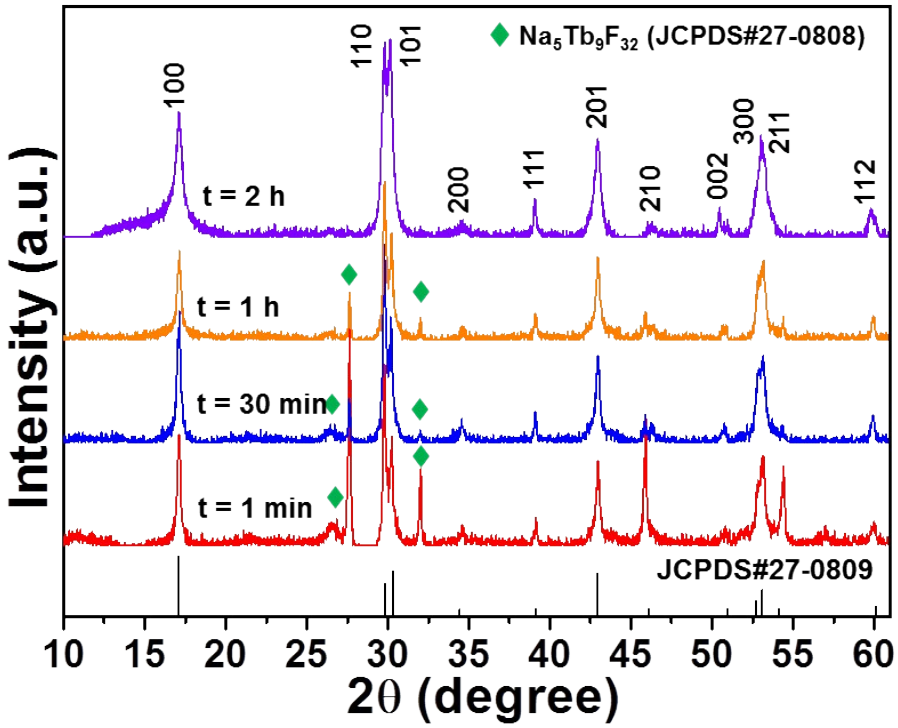

Figure S2. XRD patterns of the resultant samples synthesized at room temperature with diverse reaction time.

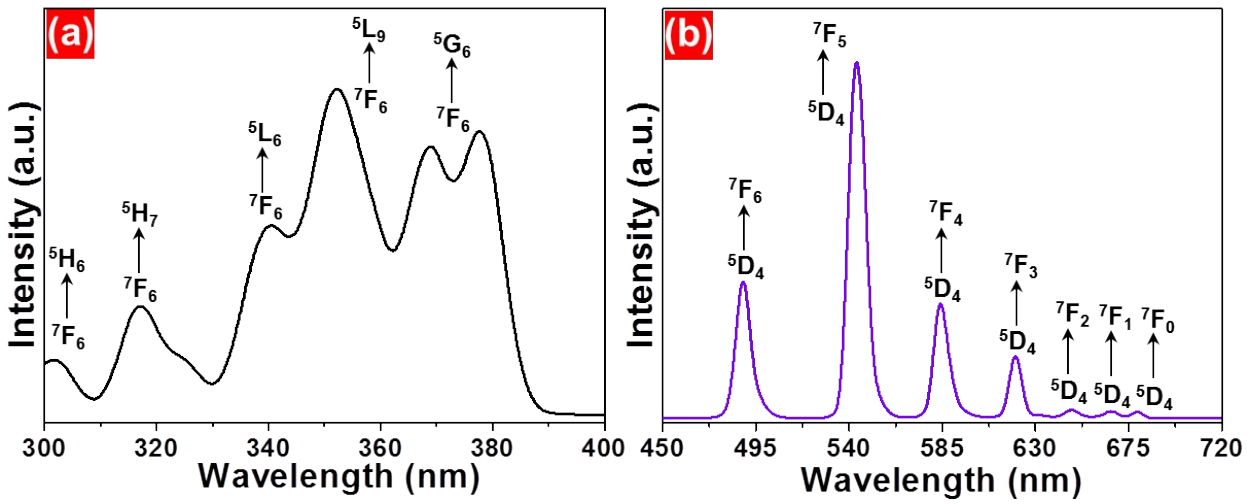

Figure S3. (a) PLE (λ_{em} = 543 nm) and (b) PL emission (λ_{ex} = 352 nm) spectra of the $NaTbF_4$ nanorods.

The photoluminescence (PL) behaviors of the $NaTbF_4$ nanorods obtained at the reaction time of 2 h were characterized by utilizing the PL excitation (PLE) and PL emission spectra. The PLE spectrum, which monitored at 543 nm, in the wavelength range of 300-400 nm consisted of five narrow peaks at around 302 nm ($^7F_6 \rightarrow {}^5H_6$), 317 nm ($^7F_6 \rightarrow {}^5H_7$), 340 nm ($^7F_6 \rightarrow {}^5L_6$), 352 nm ($^7F_6 \rightarrow {}^5L_9$) and 378 nm ($^7F_6 \rightarrow {}^5G_6$), as illustrated in Fig. S3(a), implying that $NaTbF_4$ nanorods exhibited a strong absorption in NUV light region.[1] Since the excitation band at 352 nm was much higher than other bands, we selected it as the excitation lighting source for the $NaTbF_4$ nanorods. Under the excitation of 352 nm, the PL emission spectrum was monitored and it is found to be composed of several sharp bands in which the green emission at around 543 nm arising from the $^5D_4 \rightarrow {}^7F_5$ intra-4f transition of Tb^{3+} ions took the domination in the PL emission spectrum (see Fig. S3(b)).[2] Furthermore, the other emission bands located at around 489 nm, 584 nm, 620 nm, 648 nm, 667 nm and 679 nm, which were assigned to the $^5D_4 \rightarrow {}^7F_6$, $^5D_4 \rightarrow {}^7F_4$, $^5D_4 \rightarrow {}^7F_3$, $^5D_4 \rightarrow {}^7F_2$, $^5D_4 \rightarrow {}^7F_1$ and $^5D_4 \rightarrow {}^7F_0$, transitions of Tb^{3+} ions, respectively.[2] These results suggested that the $NaTbF_4$ nanorods had good luminescent performance.

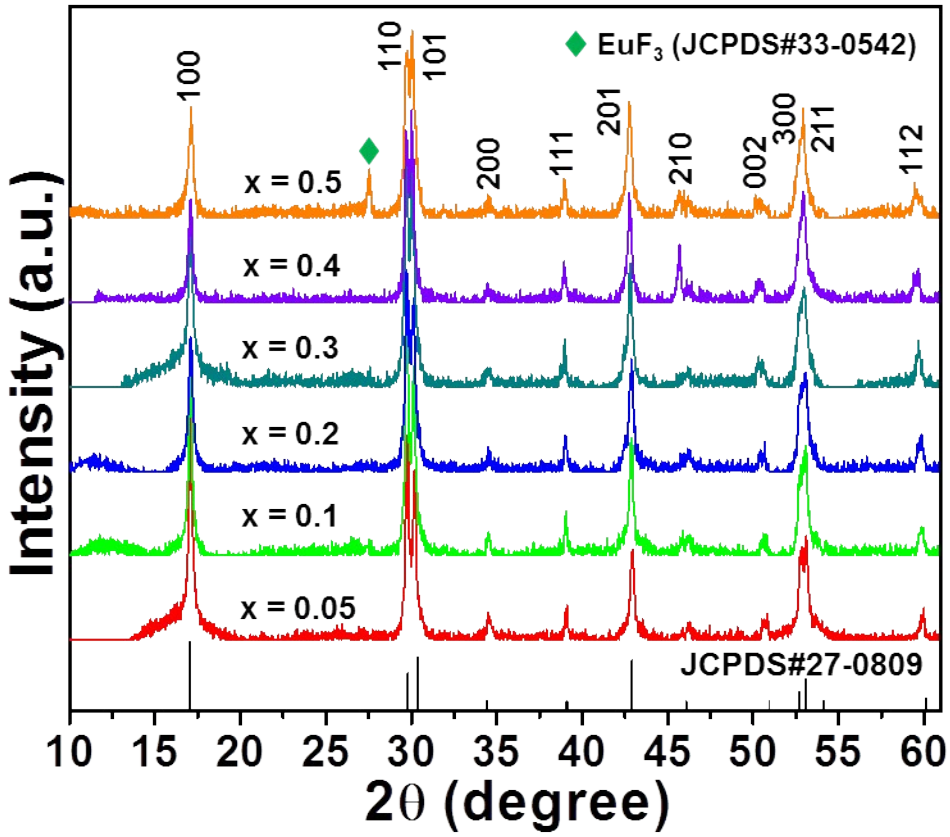

Figure S4. XRD patterns of the $NaTbF_4$:$x$$Eu^{3+}$ nanorods with various doping concentration.

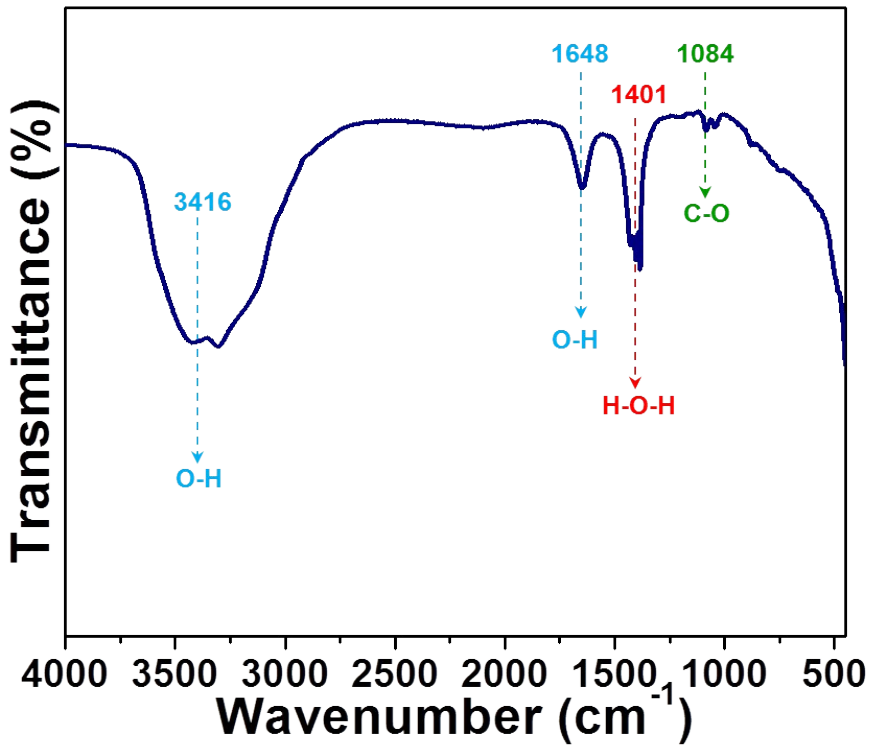

Figure S5. FT-IR spectrum of the $NaTbF_4$:0.3Eu^{3+} nanorods in the range of 450-4000 cm^{-1}.

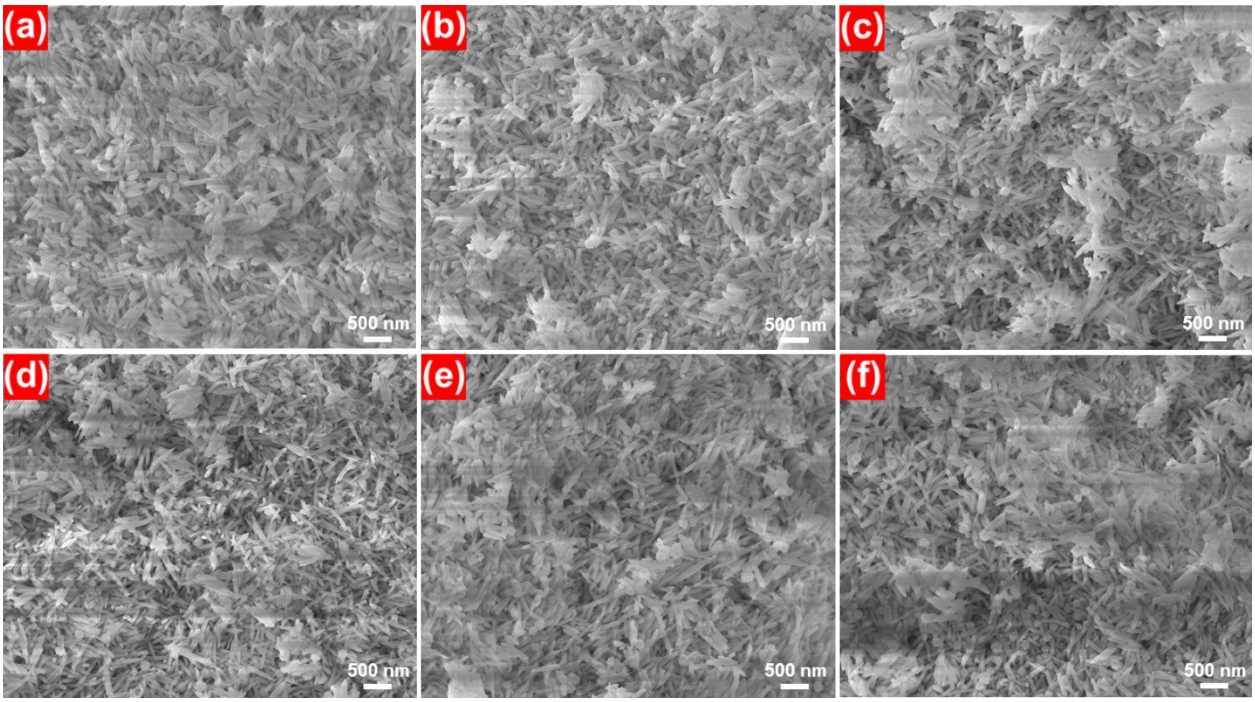

Figure S6. FE-SEM images of $NaTbF_4$:$x$$Eu^{3+}$ nanorods with different Eu^{3+} ion concentrations of (a) x = 0.05, (b) x = 0.1, (c) x = 0.2, (d) x = 0.3, (e) x = 0.4 and (f) x = 0.5.

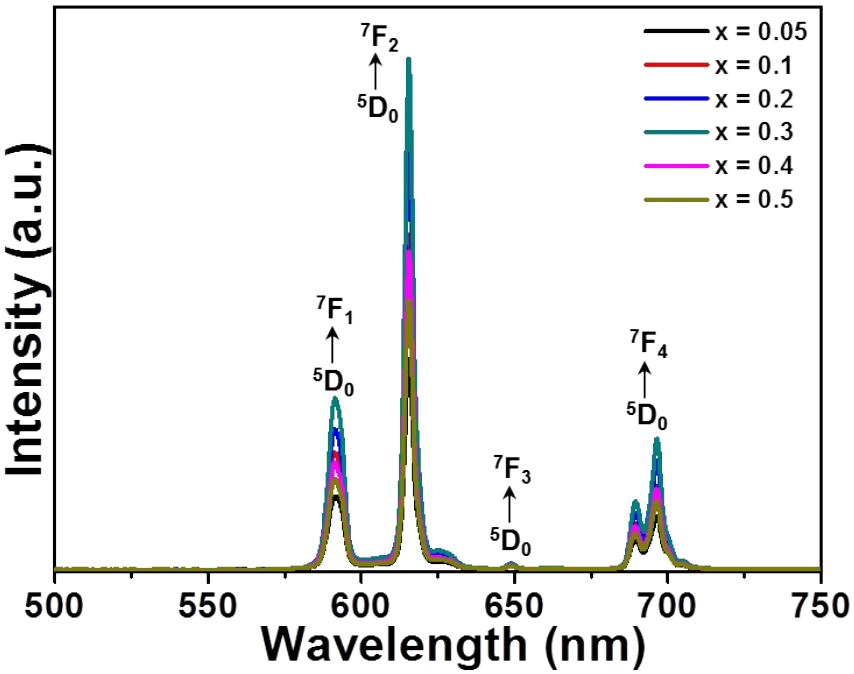

Figure S7. Room temperature emission spectra the $NaTbF_4$:$x$$Eu^{3+}$ (x = 0.05, 0.1, 0.2, 0.3, 0.4, 0.5) nanorods excited at 394 nm.

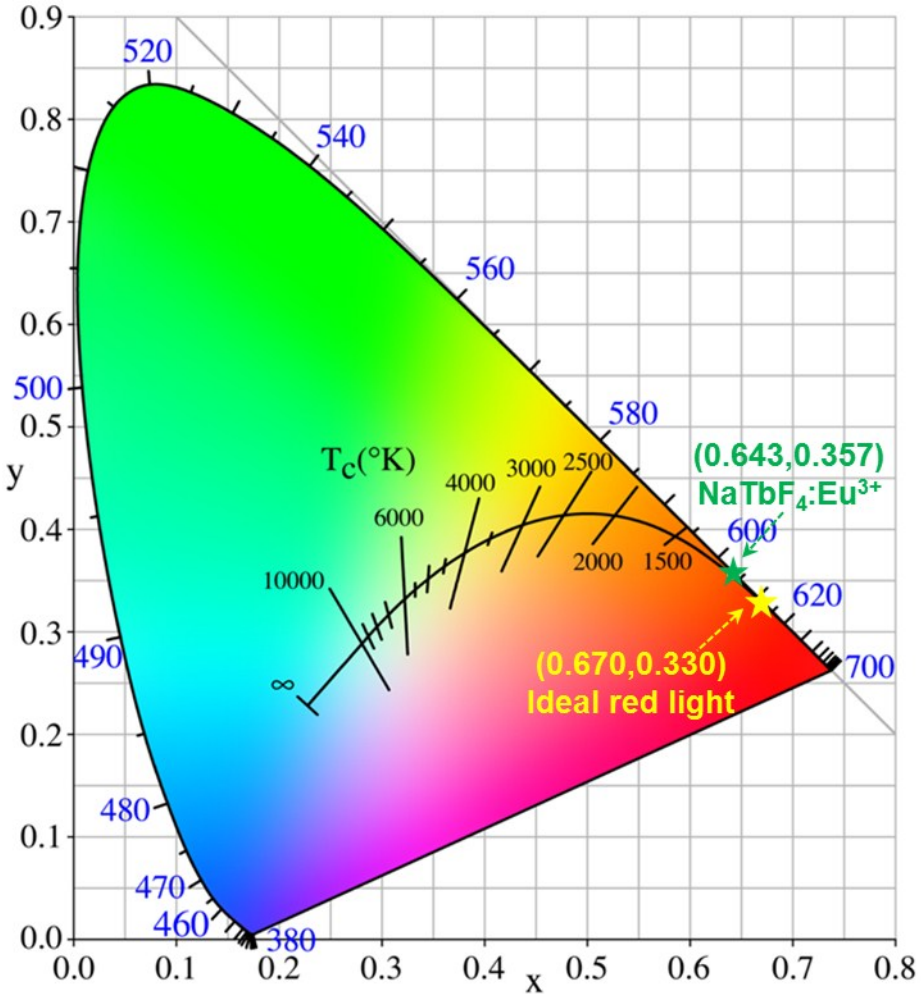

Figure S8. CIE chromaticity diagram of the $NaTbF_4$:0.3Eu^{3+} nanorods as well as the ideal red light.

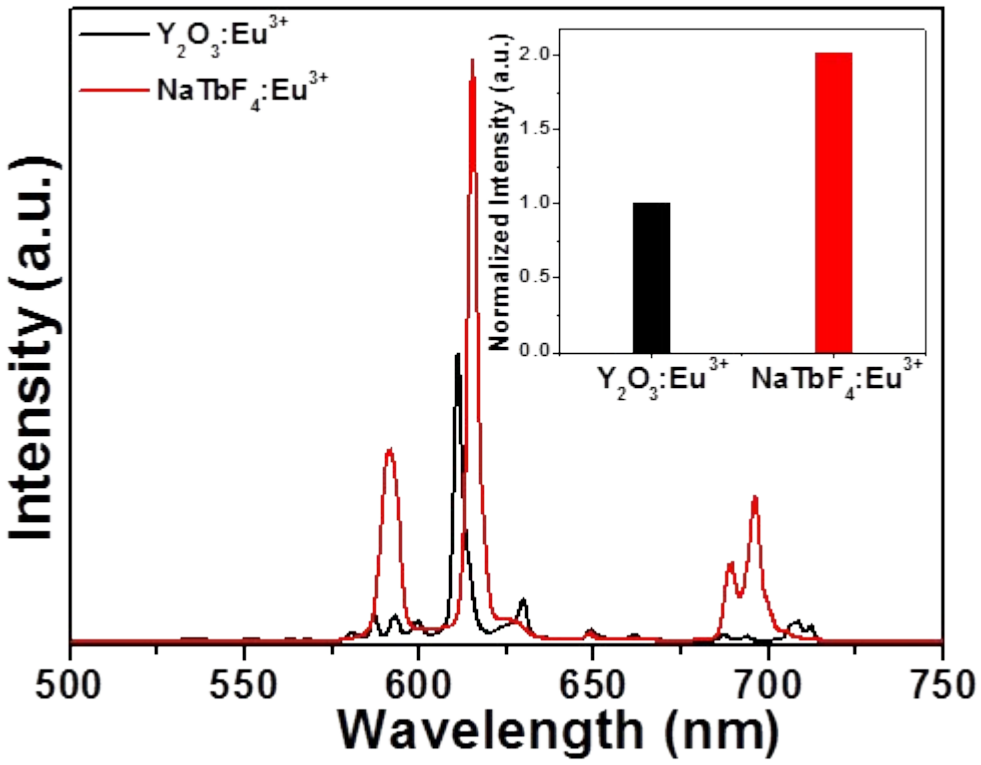

Figure S9. Comparison of the emission spectra between the commercial $Y_2O_3:Eu^{3+}$ red-emitting phosphors and resultant $NaTbF_4:0.3Eu^{3+}$ nanorods excited at the wavelength of 394 nm. Inset shows the emission intensity of $Y_2O_3:Eu^{3+}$ red-emitting phosphors and resultant $NaTbF_4$ nanorods.

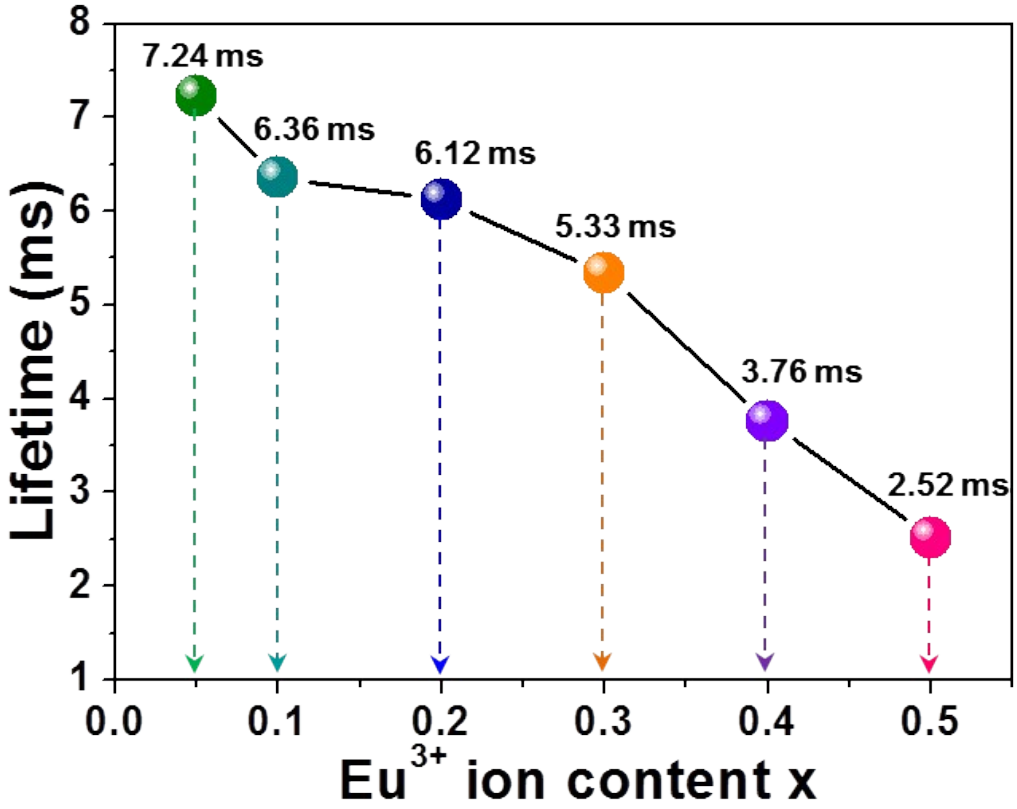

Figure S10. Dependence of lifetime on the Eu^{3+} ion concentration for the $NaTbF_4$:$x$$Eu^{3+}$ nanorods.

Since the emission intensity of red emission was much stronger than that of the yellow emission, we can deduce that the sites, which were populated by the Eu^{3+} ions in the selected host lattices, exhibited low symmetry. As a proof of the above inference, the optical transition parameters of Ω_λ (λ = 2, 4, 6) were estimated though a theoretical discussion based on the Judd-Ofelt theory. Considering the entire nanorods showed the same luminescent profiles (see Fig. S7), the $NaTbF_4$:0.3Eu^{3+} nanorods with the strongest emission intensity were selected as the typical sample to analyze the optical transition performance of dopants. From previous reports,[3,4] it is evident that the relation between total emission intensity and radiative transition ratio can be expressed as:

$$I = \sum_{J=1,2,3,4} I_{^7F_J} = \alpha \sum_{J=1,2,3,4} A_{^7F_J}, \qquad (1)$$

where $A_{7_{F_J}}$ and $I_{7_{F_J}}$ are associated with the radiative transition ratio and emission intensity of the $^5D_0 \rightarrow {}^7F_J$ (J = 1, 2, 3, 4) transition, respectively, and α denotes the coefficient. Besides, the total radiative transition rate can be calculated from the lifetime by the following expression:[3,4]

$$\sum_{J=1,2,3,4} A_{7_{F_J}} = 1/\tau \quad , \qquad (2)$$

As shown in Fig. S10, one knows that the lifetime of the synthesized $NaTbF_4$:0.3Eu^{3+} nanorods was 5.33 ms. Thus, with the aid of Eq. (1) and Eq. (2), we know that the value of α was 232.81. Moreover, according to the expression of $I_{7_{F_J}} = \alpha A_{7_{F_J}}$, the radiative transition rate for the $^5D_0 \rightarrow {}^7F_J$ (J = 1, 2, 3, 4) transition can be obtained and the corresponding results are listed in Table S2.

Obviously, the $^5D_0 \rightarrow {}^7F_1$ transition corresponds to the magnetic transition and its emission intensity is hardly affected by the local crystal field surrounding the Eu^{3+} ions. From Judd-Ofelt theory, one obtains that the radiative transition ratio of the magnetic transition of $^5D_0 \rightarrow {}^7F_1$ can be defined as:[5,6]

$$A_{J\rightarrow J'}^{MD} = \frac{64\pi^4 v^3}{3h(2J+1)} n^3 S_{MD} \quad , \qquad (3)$$

where v shows the center wavenumber of the $^5D_0 \rightarrow {}^7F_1$ magnetic transition, h is ascribed to the Planck constant with a fixed value of 6.626×10^{-27} erg s, n presents the refractive index of the studied product and S_{MD}, which exhibits a fixed value of 7.83×10^{-42}, is assigned to the magnetic dipole strength. Based on the calculated radiative transition rate listed in Table S2 and Eq. (3), the refractive index of the synthesized $NaTbF_4$:0.3Eu^{3+} nanorods was determined to be around 1.49. On the other hand, the radiative transition ratio of the $^5D_0 \rightarrow {}^7F_J$ (J = 2, 4, 6) electric dipole transition of the Eu^{3+} ions can be calculated from the following expression given by Judd and Oflet:[5,6]

$$A_{J\rightarrow J'}^{ED} = \frac{64\pi^4 v^3 e^2}{3h(2J+1)} \frac{n(n^2+2)^2}{9} \Omega_\lambda \langle \psi J \| U^\lambda \| \psi' J' \rangle^2 \quad , \qquad (4)$$

In this expression, e, which shows a fixed value of 4.8×10^{-10} esu, is the elementary charge, Ω_λ is attributed to the intensity parameter and $\langle \psi J \| U^\lambda \| \psi' J' \rangle^2$ is assigned to the reduced matrix element for the electric dipole transitions of $J \rightarrow J'$, specially, when J' = 2 and 4, its value is 0.0032 and 0.0023, respectively. From the measured emission spectra, it is evident that the emissions arising

from $^5D_0 \rightarrow {}^7F_2$ and $^5D_0 \rightarrow {}^7F_4$ transitions were observed, whereas the emission from the $^5D_0 \rightarrow {}^7F_6$ transition was not detected. Thus, in present work, we can only evaluate the values of Ω_2 and Ω_4, while Ω_6 value is impossible to be achieved. According to Eq. (9) along with the estimated radiative transition rate listed in Table S2, we found that the Ω_2 and Ω_4 values were 4.01×10^{-20} cm^{-2} and 2.06×10^{-20} cm^{-2}, respectively. Among these two parameters, the optical transition parameter of Ω_2 has been verified to be related to the asymmetry characteristic surrounding the dopant ions sites, whereas the intensity parameter of Ω_4 is associated with the bulk performance.[7,8] Particularly, Ω_2 will be larger than Ω_4 when the dopants occupy the sites with low symmetry, otherwise, Ω_4 will be larger than Ω_2 when the dopants take up the high symmetry positions in the studied host lattices.[7,8] Clearly, the evaluated Ω_2 value was much higher than Ω_4 value, implying that the site symmetry, which was occupied by the Eu^{3+} ions in the $NaTbF_4$ host lattices, was low. This theoretical calculation result coincided well with the above deduction achieving from the emission spectrum.

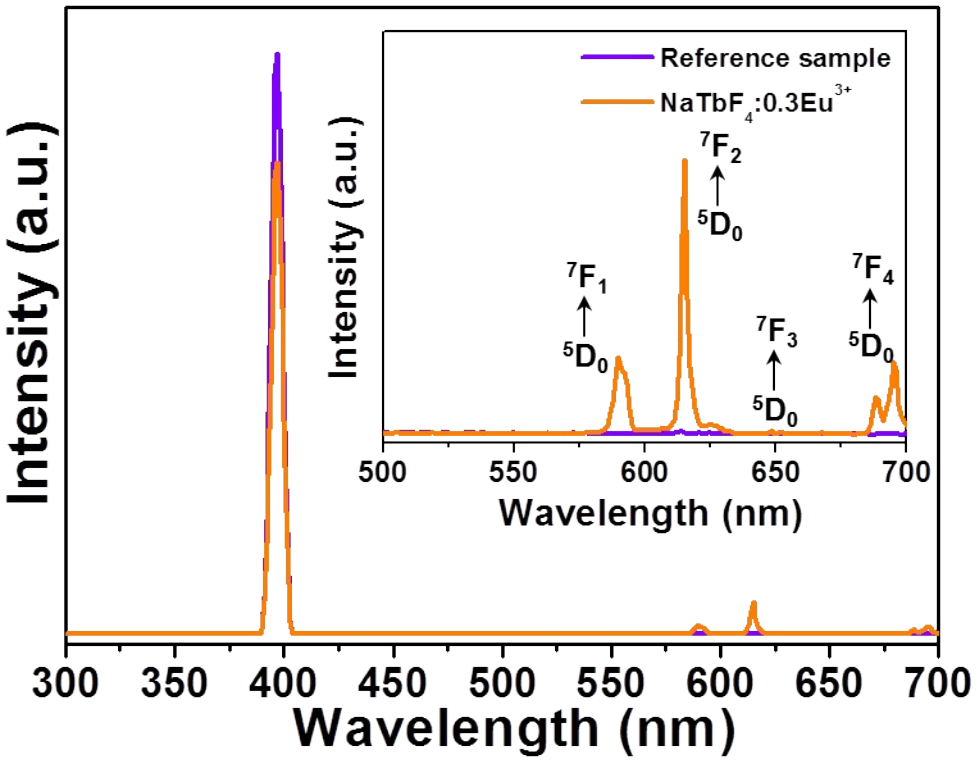

Figure S11. PL excitation and emission spectra of the $NaTbF_4$:0.3Eu^{3+} nanorods and reference sample, measured by using a spectrofluorometer attached with an integrating sphere for quantum efficiency measurement. Inset shows the magnified emission spectra in the wavelength range of 500-700 nm.

To examine the internal quantum efficiency of the designed samples, the photoluminescence excitation (PLE) and emission spectra of the $NaTbF_4$:0.3Eu^{3+} nanorods and reference samples were measured, as shown in Fig. S11. With the aid of following formula, the internal quantum efficiency was estimated:

$$\eta = \frac{\int L_S}{\int E_R - \int E_S} \times 100\% \quad , \qquad (4)$$

In this expression, η is the internal quantum efficiency, L_S shows the PL emission spectrum of the studied samples, E_R and E_S present the excitation spectra of the excitation light with and without synthesized compounds, respectively. As a consequence, based on the detected luminescent spectra along with Eq. (4), the internal quantum efficiency of the $NaTbF_4$:0.3Eu^{3+} nanorods was found to be around 50.2%.

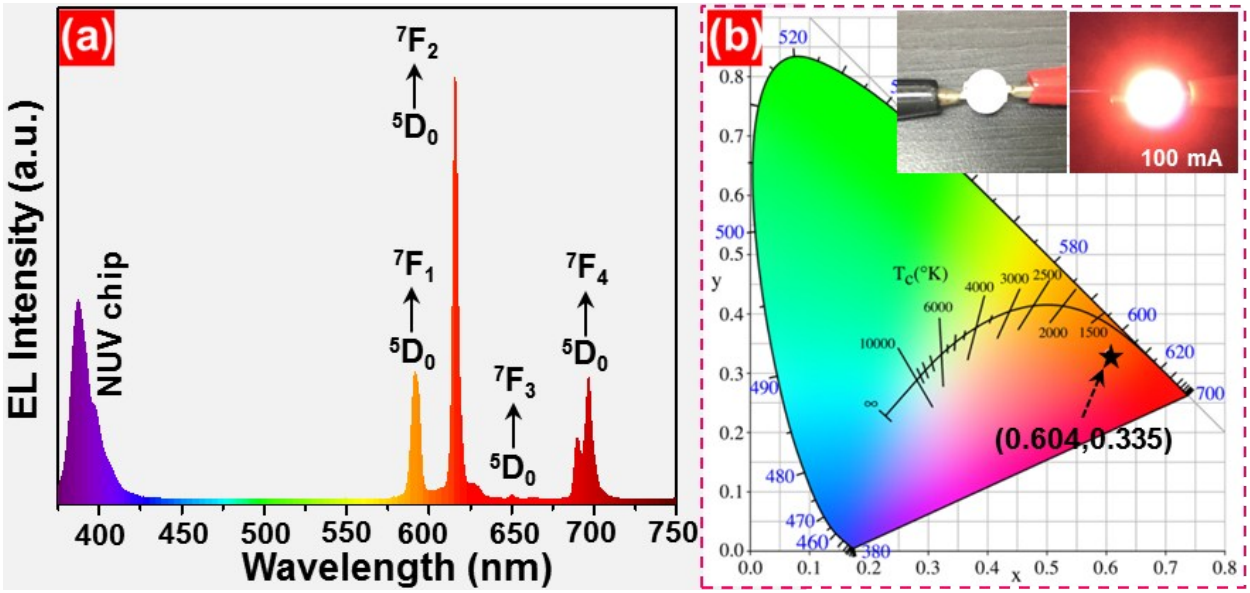

Figure S12. (a) EL emission spectrum of the developed red-emitting LED device. (b) CIE chromaticity diagram of the developed red-emitting LED device. Inset shows the luminescent images of the developed LED device without and with injection current.

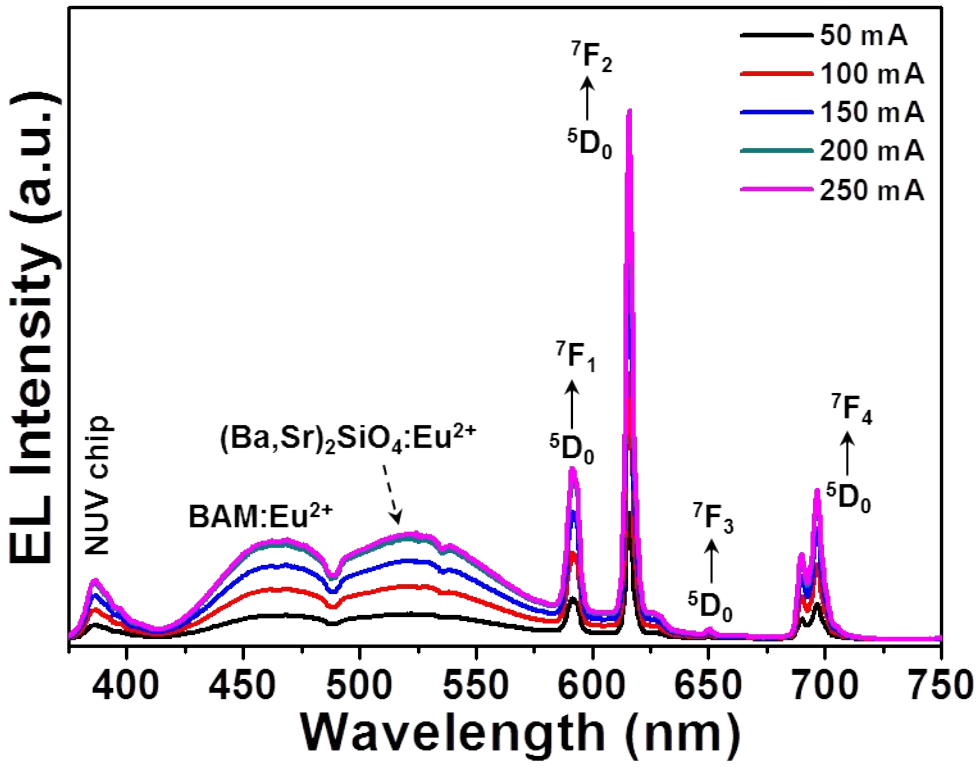

Figure S13. EL emission spectra of synthesized white-LED device as a function of injection current in the range of 50-250 mA.

Reference

1. P. Du, Y. Hua, J. S. Yu, Room-temperature synthesis of near-ultraviolet light-excited Tb^{3+}-doped $NaBiF_4$ green-emitting nanoparticles for solid-state lighting, RSC Adv., 8 (2018) 26676-26681.

2. J. Yang, H. Wu, L. Song, X. Wang, J. Dong, S. Gan, L. Zou, A novel synthesis route to monodisperse $Na_5Lu_9F_{32}:Tb^{3+}$ phosphors with superior thermal stability, J. Lumin., 204 (2018) 533-538.

3. Y. Tian, B. Chen, R. Hua, J. Sun, L. Cheng, H. Zhong, X. Li, J. Zhang, Y. Zheng, T. Yu, L. Huang, H. Yu, Optical transition, electron-phonon coupling and fluorescent quenching of $La_2(MoO_4)_3:Eu^{3+}$ phosphor, J. Appl. Phys., 109 (2011) 053511.

4. L. Wang, W. Guo, Y. Tian, P. Huang, Q. Shi, C. Cui, High luminescent brightness and thermal stability of red emitting $Li_3Ba_2Y_3(WO_4)_8:Eu^{3+}$ phosphor, Ceram. Int., 42 (2016) 13648-13653.

5. B. R. Judd, Optical absorption intensities of rare-earth ions, Phys. Rev., 127 (1962) 750-761.

6. G. S. Ofelt, Intensities of crystal spectra of rare-earth ions, J. Chem. Phys., 37 (1962) 511-520.

7. X. Wang, C. Liu, T. Yu, X. Yan, Controlled synthesis, photoluminescence, and the quantum cutting mechanism of Eu^{3+} doped $NaYbF_4$ nanotubes, Phys. Chem. Chem. Phys., 16 (2014) 13440-13446.

8. P. Du, X. Huang, J. S. Yu, Facile synthesis of bifunctional Eu^{3+}-activated $NaBiF_4$ red-emitting nanoparticles for simultaneous white light-emitting diodes and field emission displays, Chem. Eng. J., 337 (2018) 91-100.